

Manuscript version: Author's Accepted Manuscript

The version presented in WRAP is the author's accepted manuscript and may differ from the published version or Version of Record.

Persistent WRAP URL:

<http://wrap.warwick.ac.uk/141725>

How to cite:

Please refer to published version for the most recent bibliographic citation information. If a published version is known of, the repository item page linked to above, will contain details on accessing it.

Copyright and reuse:

The Warwick Research Archive Portal (WRAP) makes this work by researchers of the University of Warwick available open access under the following conditions.

© 2020 Elsevier. Licensed under the Creative Commons Attribution-NonCommercial-NoDerivatives 4.0 International <http://creativecommons.org/licenses/by-nc-nd/4.0/>.



Publisher's statement:

Please refer to the repository item page, publisher's statement section, for further information.

For more information, please contact the WRAP Team at: wrap@warwick.ac.uk.

Techno-economic performance analysis of biofuel production and miniature electric power generation from biomass fast pyrolysis and bio-oil upgrading process.

Mobolaji B. Shemfe, Sai Gu^{*}, Panneerselvam Ranganathan

Energy and Power Engineering Division, School Of Engineering, Cranfield University, Bedford, Bedfordshire, MK43 0AL, UK.

**Corresponding author: s.gu@cranfield.ac.uk*

ABSTRACT

The techno-economic performance analysis of biomass fast pyrolysis and bio-oil upgrading processes to produce gasoline and diesel range fuels, and generate electric power is explored through process simulation. In this work, a high fidelity process model of a 72 MT/day pine wood fast pyrolysis and bio-oil upgrading plant was developed with rate based chemical reactions using Aspen Plus® process simulator. It was observed from simulation results that 1 kgs⁻¹ pine wood_{db} produced 0.66 kgs⁻¹ bio-oil, 0.19 kgs⁻¹ gas and 0.15 kgs⁻¹ char. Simulation results also show that the energy required for drying and fast pyrolysis operations can be provided from the combustion of pyrolysis by-products mainly char and non-condensable gas, with sufficient residual energy for miniature electric power generation. The intermediate bio-oil product from the fast pyrolysis process is upgraded into gasoline and diesel via a two-stage hydrotreating process, which is implemented by a pseudo first order reaction of lumped bio-oil species followed by the hydrocracking process. Simulation results indicate that about 0.2 kgs⁻¹ of gasoline and diesel range products and 96W of electric power can be produced from 1 kgs⁻¹ pine wood_{db}. The effect of initial biomass moisture content on the amount of electric power generated and the effect of biomass feed composition on product yields were also reported in this study. Aspen Process Economic Analyser® was used for equipment sizing and cost estimation for an nth plant and the product value was estimated from discounted cash flow analysis assuming the plant

operates for 20 years at a 10% annual discount rate. Economic analysis indicates that the plant will require £16.6 million of capital investment and product value is observed at £6.69/GGE. Furthermore, the effect of key process parameters on product value and the impact of electric power generation equipment on capital cost and energy efficiency were also reported in this study.

Keywords: fast pyrolysis; techno-economic analysis; process modelling; biofuel production; biomass; bio-oil upgrading.

1 INTRODUCTION

Crude oil remains the main source of transport fuel and is projected to continue to dominate the fuel market over the next three decades [1]. However, to reduce the world's dependence on crude oil due to the environmental implications of burning fossil fuels coupled with stringent regulation on carbon emission, biofuels are being rapidly deployed globally as a sustainable substitute [2-4]. Biomass can be converted into biofuels mainly via biochemical and thermochemical routes. While biochemical conversion processes have been demonstrated in commercial quantities, they are economically unsustainable and exert market pressure on food crops and biodiversity [4; 5]. On the other hand, thermochemical conversion processes, which include pyrolysis, gasification and hydrothermal liquefaction, have a great potential for producing the intermediate bio-oil required for advanced biofuels production that can compete directly with fossil fuels [3; 4]. However, the products obtained from these processes vary in physical properties and chemical composition and consequently present unique technical and economic challenges [6]. Biomass fast pyrolysis presents the best case for maximising bio-oil yields, which can then be subsequently upgraded into transport fuels [7; 8]. Fast pyrolysis entails the thermochemical decomposition of lignocellulosic biomass at temperatures typically ranging from 450 to about 650°C to produce liquid (bio-oil), solids (char and ash) and non-condensable gas (NCG) at a very short vapour residence time typically 1 – 2s [9]. Fast pyrolysis bio-oil can be upgraded into

naphtha range transport fuels via two major conventional refinery operations that have been broadly identified and reviewed in literature, which are hydroprocessing and catalytic cracking [6; 10; 11]. Hydroprocessing encompasses two main hydrogen intensive processes namely hydrotreating and hydrocracking. Hydrotreating involves the stabilization and selectively removal of oxygen from untreated pyrolysis bio-oil through its catalytic reaction with hydrogen over sulfided CoMo or NiMo supported catalysts and non-sulfided precious metal catalysts while hydrocracking involves the simultaneous scission and hydrogenation of heavy aromatic and naphthenic molecules into lighter aliphatic and aromatic molecules [6; 9; 10]. Fast pyrolysis by-products (char and NCG) can be combusted to provide all the energy required to drive the process, while the residual energy can be disposed or utilized for supplementary electric power generation [9]. Although, different fast pyrolysis reactor configurations have been demonstrated on commercial and pilot scales worldwide, the bubbling fluid bed reactor has been identified as the best in terms of ease of scalability, biomass heat transfer efficiency and relative simplicity in construction [9].

The production of transport biofuels from the fast pyrolysis of biomass is yet to be commercialised due to the expensive investment required for production and a lack of competitiveness with fossil fuels; thus this makes process modelling and simulation an indispensable tool to investigate process performance and ensuring its economic viability. Furthermore, supporting processes required for the fast pyrolysis process consisting of grinding and drying processes, which are solid processes that are currently inadequately described in available software. Therefore, a high fidelity process model is required for rigorous analysis of the whole process. In addition, existing models specify the product yield compositions for the reactor without accounting for the effect of temperature and chemical kinetics due to the complexity of the thermochemical reaction kinetics involved, and most available reaction models in literature are descriptive of the intra-particle relationship rather than predictive of the product distribution [12]. Therefore, a model that is able to predict the

process yields and process energy requirements at varying operating conditions with minimal assumptions would be necessary.

There are several studies on the techno-economic analysis of biomass fast pyrolysis for bio-oil production available in literature, with very few studies considering the upgrading of fast pyrolysis bio-oil into transportation fuels and quantifying the amount of electric power capable of being generated from fast pyrolysis by-products [13-16]. These studies report bio-oil cost ranging from US\$0.62/gal to US\$1.40/gal and capital cost ranging from US\$7.8 to US\$143 million over a 240 to 1,000 MT/day plant capacity range. The significant disparity in the bio-oil cost for these studies can be attributed to the fact that different assumptions were adopted in each study. Few researchers have conducted techno-economic analysis on biomass fast pyrolysis process for transport fuel production [17-18]. Jones *et al.* [17] conducted a design case study to evaluate the production of hydrocarbon biofuel from a 2000 MT/day plant of hybrid poplar wood chips. In this study, capital expenditure of US\$303 million was estimated with a minimum fuel selling price of US\$2.04. A techno-economic analysis was also conducted by Wright *et al.* [18] on a 2000 MT/day of corn stover fast pyrolysis plant and subsequent bio-oil upgrading via hydrotreating and hydrocracking processes to obtain fuel product value and capital costs at US\$2.11/gal/US\$287 million and US\$3.09/gal/US\$200 million for hydrogen purchase and *in-situ* hydrogen production scenarios respectively.

In this study, a 72 MT/day fast pyrolysis plant of pine wood, electric power generation from fast pyrolysis by-products and subsequent bio-oil upgrading processes are modelled based on rate based chemical reactions to evaluate the techno-economic performance of the process. Particularly, more emphasis is made on the detailed process modelling of each process equipment. The fast pyrolysis reactor model is developed based on rate based multi-step chemical reactions [19] using Aspen Plus® process simulator and validated with experimental results reported by Wang *et al.* [20]. Auxiliary processes consisting of grinding,

screening, drying, combustion, bio-oil collection system and power generation are modelled based on design specifications with the appropriate thermodynamic property methods. The hydrotreating process is modelled based on a pseudo first order reaction kinetic lumped model over Pt/Al₂O₃ catalysts [21]. Based on validated process models, the effect of process input parameters on the process and economic performance are explored.

2 MATERIAL AND METHODS

2.1 Process Description

The overall process of transportation fuel production from biomass is divided into eight main processing units described by the generalised process flow diagram in Figure 1. In the feed pre-treatment processing (A100), the feed undergoes grinding and drying operations to meet the minimum pyrolysis reactor feed requirement of 2mm diameter and 10% moisture content. Next, it is passed on to fast pyrolysis fluidized bed reactor (A200) where the biomass feed is thermochemically converted in the absence of oxygen into non-condensable gases(NCG), hot pyrolysis vapours and char at a temperature range of 450 - 500°C. The product from the reactor is fed into the solid removal section (A300), where the char is separated from the pyrolysis vapour before bio-oil is to be condensed. The condensation of pyrolysis vapours is done (A400) by quenching it into liquid in the bio-oil recovery section, which contains vapour quenching process units that separate the desired product (bio-oil) from non-condensable gases. NCG and char separated from bio-oil, are then combusted to generate the energy (hot flue gas) required for biomass drying and fast pyrolysis processes in the combustion section (A500). The residual heat from combustion, if any, is used to generate the high pressure steam for power generation (A600). The bio-oil is upgraded into gasoline and diesel fraction products in the upgrading section containing hydrotreating and hydrocracking processes (A700). Hydrogen required for hydroprocessing is generated in the hydrogen generation section (A800).

2.2 Model Development

The biomass fast pyrolysis model is implemented in Aspen Plus® V8.2 using its improved solid modelling capabilities. The main model assumptions used in this study are presented in Table 1. The comprehensive process flow diagrams for bio-oil production and electric power generation (A100-A600) and bio-oil upgrading (A700 – A800) is shown in Figures 2 and 3 respectively.

2.2.1 Pretreatment section (A100)

The wet pine wood stream (CHR-1) supplied at 20mm diameter is fed into a multiple roll crusher (CHR) in which the particle size is reduced to 2mm and followed by a screen (SCRN) for particle separation. The exiting wet biomass stream (CHR-2) with initial moisture content of 25% is then fed into a rotary dryer (DRYER) at operating temperature of 300°C to reduce its moisture content. A rotary dryer was adopted in the model due to its flexibility in operation, low maintenance costs and high operating temperature range [22]. The energy required for drying is supplied by a fraction of flue gas (DYR-FLS) from the combustor (CB-BUR) which exits the dryer as a mixture of hot air and water vapour (DR-4), while the dried pine wood exits the dryer with 10% moisture content (DR-3). The dried biomass feed then goes into the fluidised bed reactor.

2.2.2 Pyrolysis section (A200)

Three model blocks (PYR-DEC, PYR-FLD and PYR-RXN) were used to model a bubbling fluidised bed pyrolysis reactor. In the yield reactor (PYR-DEC), biomass is fragmented into its subcomponents (cellulose, hemicellulose and lignin). The fluidised bed (PYR-FLD) is used to model reactor fluid dynamics with specified bed pressure drop of 150 mbar and inert sand bed mass ratio to biomass particle at 1:1.25, and reactor temperature of 500°C by varying the fluidizing gas flowrate comprising on inert nitrogen gas (FLGAS-1). The transport disengagement height in fluidized bed is calculated using Fournol *et al.* [23] empirical correlation for FCC powders with particles classified as Geldart B particles. The process

heat and fluidizing gas for the fluid bed is supplied at 863°C with a 1:1 mass ratio to biomass feed. The rate based chemical reactions of each biomass subcomponent was modelled inside the CSTR (PYR-RXN) using multi-step reactions kinetics of biomass pyrolysis developed by Ranzi *et al.* [19]. The bio-oil vapour residence time is specified at 2s. The reactor products composing of a mixture of hot volatile vapours, gas and char is sent into a cyclone (SP-CYC) to separate the solid char (PYR-SD).

2.2.3 Products separation and recovery (A300-A400)

Char and unreacted biomass (PYR-SD) are separated from the hot vapour and gas stream (PYR-VAP) in a cyclone (PYR-CYC) at 95% separation efficiency, and the separated solids are subsequently fed into the combustor. The remaining stream of hot vapour and gas (PYR-VAP) at 500°C goes into a spray tower (QUENCH), where the hot vapours are quenched to 49°C using previously stored bio-oil liquid at 25°C (QC-LIQ) as the quench liquid with a mass ratio of 10:1 to the hot vapour stream. The spray tower is modelled using Non-random two-liquid activity coefficient model with Nothnagel equation of state as vapour phase model (NRTL-NTH). The non-condensable gas (QC-GAS) then goes into a high pressure vapour-liquid separator (DEMISTER) operated at 10 bar to collect the bio-oil vapours entrained as aerosol particles. An electrostatic precipitator (ESP) could be used instead but this was avoided due to its very high equipment cost [9]. The resultant dry non-condensable gas goes to a combustor along with char while the quenched bio-oil is sent for further upgrading.

2.2.4 Combustion section (A500)

The combustion section is modelled by a yield reactor (CB-DEC) and a Gibb's reactor (CB-BUR). Unreacted biomass separated from the cyclone goes into the yield reactor (CB-DEC) to decompose into its constituent elements before it is fed into along with char (assumed to be 100% carbon in elemental constitution) and non-condensable gas (NCG) into the Gibb's reactor (CB-BUR), which calculates multi-phase chemical equilibrium by minimizing Gibb's free energy and was modelled using Peng-Robinson-Boston-Mathias (PR-BM) equation of

state. The fuel mixture of solids and NCG are combusted in 60% theoretical air at combustion temperature of 1269°C in order to mitigate ash melting and prevent material failure at severe temperatures, although a maximum temperature of 1700°C can be achieved at complete combustion. Ash is separated from the resultant combustion gases by hot cyclone (ASH-SEP). The resultant flue gas (FL-GAS) is sent into a splitter (GAS-SPLIT), where it is divided into two streams: (PYR-FLGS) and (DRY-FLGS). These are supplying heat for the feed nitrogen gas, which goes to the fluidized bed pyrolysis reactor and for the feed air, which goes to dryer via two-steam heat exchangers. The residual flue gas heat at 800°C is used for superheated steam generation for subsequent electric power generation.

2.2.5 Power generation (A600)

The residual heat generated in the combustion process is exchanged with water in a two-stream heat exchanger to generate superheated steam at 450°C and 50bar with an outlet flue gas temperature at 90°C. The superheated steam is supplied to a steam turbine (TURB), modelled at 75% isentropic efficiency and turbine efficiency of 85% to generate electricity (P3).

2.2.6 Bio-oil upgrading (A700)

Bio-oil product (BIO-OIL) is hydrotreated in a two-stage hydrotreating process over Pt/Al₂O₃ catalyst due to increased aromatic yield compared with conventional catalysts such as sulfided CoMo/Al₂O₃ and sulfided Ni-Mo/Al₂O₃ [21]. Two hydrotreaters were considered and modelled by two CSTRs (HDO1 and HDO2) using a pseudo first order reaction kinetic model of lumped species based on previously reported study [21]. A yield reactor was introduced afore the hydrotreaters to lump bio-oil into five pseudo-components namely light non-volatile; heavy non-volatile; phenolics; aromatics + alkanes; Coke + H₂O + outlet gases. Since all chemical compounds in the bio-oil are primarily composed of carbon, hydrogen and oxygen, the pseudo components are grouped solely based on their molecular weights. The lumped bio-oil species goes into the first hydrotreater (HDO-1) operating at mild conditions 270°C

and 87bar and then fed into the second hydrotreating unit (HDO-2) under more severe operating temperature 383 °C and 87bar in a hydrogen-rich environment of about 5 wt. % [24]. The weight hourly space velocity (WHSV) for the reactors is specified as 2 hr⁻¹. The hydrotreater product (HO-P) is sent into a flash drum (F-DRUM) operated at 40°C and 20 bar to separate hydrotreater gas (HO-VP) from hydrotreated oil (HO-LQ). Hydrotreated oil goes into a phase separator to separate the polar phase from the non-polar phase; with the former going into a reformer to generate hydrogen and the latter fed to a hydrocracker (HYD-CYC) to obtain gasoline and diesel range fuels. Due to lack of adequate knowledge of bio-oil hydrocracking reaction kinetics, a yield reactor was adopted for modelling the unit, and yields are specified based on hydrocracking product oil composition from the work conducted by Elliot *et al* [25]. The hydrocrackates are finally separated into gasoline and diesel products in a naphtha splitter (SPLITTER).

2.2.7 Hydrogen production (A800)

The aqueous phase reforming unit entails two reactors: a pre-reformer modelled with a yield reactor (PRFM) and an aqueous phase reformer (APR) represented by a Gibbs reactor based on UOP bio-oil aqueous reforming process scheme [24]. The pre-reformer is operated at 260°C to generate synthesis gas, which is subsequently fed to the aqueous reformer along with supplementary natural gas to undergo equilibrium reforming reactions with superheated steam supplied at 500°C. The aqueous reformer modelled by a Gibb's reactor Peng-Robinson-Boston-Mathias (PR-BM) thermodynamic property method calculates the reforming phase and chemical equilibrium reactions by minimizes Gibbs free energy with the products specified as CO, H₂, CO₂ and H₂O. The target hydrogen product flowrate is specified by varying the flowrate of superheated steam required in the reformer using a design specification block. The product from the aqueous reformer goes into a flash drum where the gas mixture is separated from water and then the gas mixture is sent to a pressure swing adsorption (PSA) unit which separates hydrogen from the gas mixture.

2.3 Process Economics

Equipment cost estimation and sizing is conducted in Aspen Process Economic Analyser® V8.2 (APEA) based on Q1. 2013 cost data. APEA maps unit operations from Aspen Plus® flowsheet to equipment cost models, which in turn size them based on relevant design codes, and estimate the Purchased Equipment Costs (C_{PE}), and Total Direct Costs (C_{TDC}) based on vendor quotes. The cost of the equipment that cannot be estimated from APEA, are estimated from the cost equation below using costs from Wright *et al* [18] as the basis for estimation.

$$C_1 = C_o * \left(\frac{S_1}{S_o}\right)^n \quad (1)$$

Where C_1 is the new estimated cost with S_1 capacity, C_o is the initial equipment cost with S_o capacity and n is the scaling factor typically 0.6. The hypothetical plant is situated in North-Western England, hence material costs and wage rates from the UK are applied, and costs are given in Pound Sterling. The capital investment estimation methodology adopted in this study for the n^{th} plant scenario is illustrated in Figure 4. Total Indirect Cost (C_{TIDC}), which includes design and engineering costs, and contractor's fees, is taken as 20% of C_{PE} . Project Contingency (PC) is taken as 20% of the sum of Total Direct and Indirect Costs. Total Fixed Capital Investment (C_{TFCI}) is estimated from the sum of C_{TDC} , C_{TIDC} and PC, and Total Capital Investment (C_{TCI}) is estimated from the summation of working capital (5% of C_{TFCI}) and C_{TFCI} .

Total operating cost is also estimated from APEA, considering various costs including operating labour cost, raw material cost, hydroprocessing catalyst cost, reformer catalyst cost, PSA packing, ash disposal cost, maintenance cost, utilities cost, operating charges, capital charges, plant overhead, and general and administration (G & A) costs. For discounted cash flow (DCF) analysis, the following investment parameters are assumed: tax

rate of 40%; required rate of return (RRR) 10% and 20 years project economic life. The main economic inputs and assumptions adopted for economic analysis are presented in Table 2.

2.4 Model Inputs

The model inputs including proximate analysis of pine wood and biomass subcomponent composition are shown in Table 3. Multi-step reaction kinetics of biomass pyrolysis as shown in Figure 5 was implemented in this work. Bio-oil hydrotreating reaction kinetics was implemented by lumping approach of bio-oil components, which is shown in Figure 6. The kinetic parameters for biomass pyrolysis and bio-oil hydrotreating reactions are given in Tables 4 and 5 respectively.

3 RESULTS AND DISCUSSION

3.1 Model Validation

Experimental work by Wang *et al.* [20] on a fluidized bed pyrolysis reactor using pine wood is used to validate the fast pyrolysis reactor model developed in Aspen Plus®. The fast pyrolysis reactor model result and experiment data at 500°C reactor temperature are presented in Table 6, which indicate that the gas, bio-oil and char yields of the model agree with reported experimental data, and is consistent with pyrolysis product distribution reported in literature [7-9]. Furthermore, the comparison between fast pyrolysis reactor model prediction and experimental measurements of pyrolysis products as function of reaction temperature is depicted in Figure 7.

It is found that pyrolysis reaction model results agree considerably with experimental data, particularly between 475 and 550°C which is the typical temperature range at which bio-oil yield is highest. The hydrotreating reactor model result was validated with experimental work by Sheu *et al.* [21] at 400°C reaction temperature, 87.2 bar pressure and WHSV of 2hr⁻¹ over Pt/Al₂O₃ catalyst as shown in Table 7. It can be seen from the Table 7 that hydrotreating

model results are in adequate agreement with experimental data. The summary of simulation results from the validated model is presented in the in Table 8.

The moisture content of the biomass feed after undergoing drying operation is reduced to 10% with the remainder purged as dryer exhaust with 499 kg/hr as water vapour. The product yield for non-condensable gas, bio-oil and char produced from the process is 12 wt. %, 66 wt. % and 22 wt. % respectively. These values are comparable to previously published studies [7-9]. The amount of water in the bio-oil product is 20 wt. %, which is 31% more than the moisture remaining in the biomass after drying. The increase in moisture content in the bio-oil product can be attributed to the water generated during pyrolysis reactions. The combustible non-condensable gases produced mainly consist of H₂, CH₄, C₂H₄, CO and trace amounts of light volatile organic alcohols and aldehydes which collectively account for 64 wt. % while CO₂ make up 35 wt. % of the gas. Residual solids from the pyrolysis process mainly consist of char (100% carbon) and unreacted biomass. The hydrotreated bio-oil generates 31 wt. % long chained aromatics, phenolics and aliphatic compounds which are subsequently hydrocracked into smaller hydrocarbon molecules.

3.2 Energy Efficiency

In order to estimate the energy efficiency effectively, the whole process is divided into two main sub-processes: biomass pyrolysis process (drying, fast pyrolysis and electric power generation) and bio-oil upgrading process (hydrotreating, hydrocracking and aqueous reforming).

3.2.1 Energy efficiency of fast pyrolysis process

The total energy input (E_B) into the biomass pyrolysis process is estimated from the energy content in pine wood of 25 wt.% wet basis in terms of its calorific value [26] and mass flow rate, which is about 11.32MW. The electricity input requirement (W_{input}) required for dryer air blower, pyrolysis air blower, compressors and bio-oil pumps is 0.08MW. The energy

content (E_{BO}) of fast pyrolysis bio-oil in terms of its $HHV_{\text{bio-oil}}$ [9] and mass flow rate, is estimated to be 7.56MW. Furthermore, the amount of 0.24MW of electric power is generated from the steam cycle (W_{HE}).

The efficiency of fast pyrolysis without electricity generation, η_p , is determined as:

$$\frac{E_{BO}}{E_B + W_{Input}} = 66.3\%$$

Next, the net electrical efficiency η_{el} is determined as:

$$\frac{W_{HE}}{E_B + W_{Input}} = 2.1\%$$

The overall energy efficiency of the fast pyrolysis process with electric power generation, η_{pel} , is determined as: $\eta_p + \eta_{el} = 68.4\%$

The energy efficiency of the process without electric power generation is 66.3% which increased by 2.1% when a steam cycle is integrated with the fast pyrolysis process to generate electricity. However, the marginal increase in efficiency as a result of power generation may not be sufficient to justify the additional investment in power generation equipment.

3.2.2 Energy efficiency of bio-oil upgrading process

Energy content (E_{Bo}) in pyrolysis bio-oil is 7.56MW and energy content of supplementary natural gas ($E_{N.G}$) fed to the aqueous reformer is 0.35MW. The electricity input requirement (W_{input}) required for upgrading process pumps and compressors is 0.1MW. The energy content (E_{Fuel}) of the product biofuel is 6MW. Thus, local energy efficiency of the bio-oil upgrading process is 75%, and the overall energy efficiency of the process of converting biomass into biofuel products and electric power is 52.8%.

3.3 Effect of Feed Composition

Various biomass feeds were compared with pine wood to examine the effect of feed composition on fast pyrolysis products and biofuel yields. The composition of various biomasses used in the comparative simulation is shown in Table 9. The effect of the biomass composition on fast pyrolysis products and biofuel yield is presented in Figure 8. It was observed that poplar wood has the highest bio-oil yield at 68 wt. % while pine bark has the lowest bio-oil yield at 57 wt. %. This could be attributed due to fact that the composition of cellulose in polar wood is higher than that in pine bark, which in turn results in significant variation in the amount of fuel produced from each biomass as the highest fuel yield is observed for poplar at 31 wt. % of bio-oil produced, and the lowest fuel yield observed for pine bark at 27 wt. % of bio-oil produced. The non-condensable gas yield follow an opposite pattern with the highest yield at 25 wt. % for pine bark and lowest yield of 18 wt. % for poplar. Also, the highest char yield is obtained from pine bark at 18 wt. % and the lowest char yield was observed for poplar at 13.wt%.

The amount of electricity generated from each biomass was also investigated, and is depicted in Figure 9. The highest electricity of 0.38MW is generated from pine bark while the lowest electricity of 0.21MW is generated from poplar. Thus verifying the hypothesis that lignin is the main precursor of char formation for combustion, which is higher in pine bark.

3.4 Effect of Initial Biomass Moisture Content

The initial moisture content in biomass has no significant effect on product yields as it is reduced to 10% prior to its entry into the pyrolysis reactor but it has an effect on the amount of combustor flue gas available for electric power generation. The impact of the initial moisture content in the biomass feed on the amount of power generated from the process is explored, by varying moisture content between 20 and 30 wt. %. As expected the higher the initial moisture content in the biomass more energy is required to reduce its moisture content

to 10% moisture content requirement in the pyrolysis reactor. The effect of the initial moisture content in biomass on the amount of heat available for power generation is depicted in Figure 10, implying that the initial moisture content of the biomass has an effect on the overall efficiency of the process.

3.5 Economic Analysis

3.5.1 Economic results

Total Capital Investment (C_{TCI}) for the 72MT/day pine wood fast pyrolysis, bio-oil upgrading and hydrogen production plant is estimated at £16.6 million, which accrues from the summation total direct cost (C_{TDC}), indirect cost (C_{TIDC}), project contingency at 20% of total direct and indirect costs, and working capital. The percentage of contribution to C_{TCI} from the two main sub-processes including the fast pyrolysis and bio-oil upgrading is presented in Figure 11. The result indicates that the upgrading process accounts for 61% of Total Capital Investment at £10 million, while the pyrolysis accounts for the remaining 39% at £6.6 million.

The proportion of C_{TCI} for various process units in fast pyrolysis process is illustrated in Figure 12. Result indicates that the pyrolysis and pre-treatment sections account for most of the capital investment required for the fast pyrolysis process, which are about 2.48 and 2.08 £MM respectively while char separation and combustion contribute the lowest to C_{TCI} in the fast pyrolysis sub-process i.e. 0.07 and 0.26 £MM respectively.

The result of the economic analysis is presented in Table 10. Annual operating cost for the plant is estimated at £6.4 million which accounts for operating labour cost, maintenance cost, and supervision cost, utilities cost and raw material cost. In addition, catalysts replacement cost of £7.6 million is applied in the first and tenth production years assuming a 10 year catalyst lifespan. Hydrocarbon (gasoline and diesel) fuel yield for the plant is 1.8 million gallon per year and electric power generated per annum is 2.01 GWh. Income is generated from the sales of hydrocarbon fuels and excess electricity produced. Electricity

price is assumed at £0.15/kWh based on average market rates [26]. The fuel product value (PV) is obtained at zero Net Present Value (NPV) based on a 10% discount rate. Product value for this plant is observed at £6.69 per GGE when the NPV is zero.

3.5.2 Sensitivity analysis

To evaluate the effect of changes in process parameters on the project viability, a sensitivity analysis was conducted over a $\pm 20\%$ range by varying fuel yield, operating cost, electricity generated and capital investment as shown in Figures 13 and 14. Sensitivity analysis indicates that the product value (PV) shows the highest sensitivity to variation in fuel yield; 10% and 20% increase in fuel yield result in 9% and 17% decrease in product value respectively, showing a positive impact on the project economic viability. Conversely, 10% and 20% decrease in fuel yield result in 11% and 25% increase in the product value of the project, which in other words signifies a negative impact on the economic viability of the project. Operating cost shows the second highest sensitivity to PV with 10% and 20% increase in operating cost resulting in 7% and 15% increase in PV respectively and *vice versa*. 10% and 20% increase in tax result in 7.34% and 7.66% increase in PV respectively. Conversely, a decrease in tax shows a more rapid impact on PV; 10% and 20% decrease in tax result in 6.40% and 12.06% decrease in PV respectively.

Variation in capital investment indicates a relatively marginal impact on PV, with 10% and 20% increase in capital investment resulting in 1.4% and 3% increase in PV respectively and *vice versa*. Electricity generation indicated the lowest sensitivity to the PV, with 10% and 20% increase in electricity generated yielding minimal 0.48% and 0.90% decrease in PV respectively and *vice versa*.

4 CONCLUSIONS

A high fidelity process model of a 72 MT/day pine wood fast pyrolysis and bio-oil upgrading plant was built in Aspen Plus® and validated with experimental data from literature. Major conclusions drawn from this study are as follows:

- Simulation results indicate an overall energy efficiency of 52.8% for an integrated plant while the local energy efficiency of biomass fast pyrolysis process with and without electric power generation indicates 66.3% and 68.4% respectively. The combustion of biomass fast pyrolysis by-products (char and NCG) provides the energy required for both drying and the fast pyrolysis processes with sufficient residual energy to generate electric power.
- The inclusion of power generation equipment increase the total capital investment of the pyrolysis process by 16% whilst generating only 0.24MW which contributes 2.1% increase to energy efficiency, hence it doesn't justify additional capital investment in power generation equipment; nevertheless the amount of energy available for power generation is highly dependent of the amount of moisture in the biomass.
- The amount of moisture in the biomass has an effect of the overall energy efficiency of the process; thus a prior dried biomass is more suitable to increase the overall energy efficiency of the process. Also, process heat integration can be further explored to increase process energy efficiency by identifying possible areas of energy savings for optimised energy use.
- Economic analysis indicates that gasoline and diesel products can be produced from biomass fast pyrolysis and bio-oil upgrading at a product value of £6.69/GGE and require total capital investment and annual operating costs of £16.6 million and £6.4 million respectively based on Q1. 2013 cost year over a 20 year project cycle and a 10% annual discount rate.

- The bio-oil upgrading process contributes about 61% to total capital investment while fast pyrolysis accounts for the remaining 39%; thus further equipment optimization may be required to minimize capital cost in the upgrading process.
- Sensitivity analysis of process parameters indicates that the fuel product value is highly susceptible to changes in fuel yield, operating cost and tax while capital investment and electric power generated shows a minimal impact on product value. Since, catalyst development for upgrading bio-oil is being researched extensively, new advances in low cost catalysts to improve fuel yield will reduce the cost of production significantly. Furthermore, tax breaks from government will have a significant impact on the process commercial viability and outlook.

LIST OF ABBREVIATIONS

APEA	Aspen Process Economic Analyzer® V8.2
CSTR	Continuous stirred-tank reactor
DB	Dry Basis
DCF	Discounted cash flow
ESP	Electrostatic precipitator
GGE	Gasoline gallon equivalent
HHA	Hydroxyacetaldehyde
HHV	Higher heating value
HMFU	Hydroxymethylfurfural
HT	Hydrotreated
IRR	Internal rate of return
MM	Million
MT	Metric Ton
NCG	Non-condensable gases
NPV	Net Present Value
NRTL-NTH	Non-random two-liquid - Nothnagel
PR-BM	Peng-Robinson-Boston-Mathias

PSA	Pressure swing adsorption
PV	Product Value
RRR	Required rate of return

REFERENCES

- [1] British Petroleum. BP Energy Outlook 2030. http://www.bp.com/content/dam/bp/pdf/Energy-economics/Energy-Outlook/BP_Energy_Outlook_Booklet_2013.pdf [accessed 25/08/2014].
- [2] Demirbaş A. Biomass resource facilities and biomass conversion processing for fuels and chemicals. *Energy Conversion and Management* 2001; 42:1357-78. doi: 10.1016/S0196-8904(00)00137-0.
- [3] International Energy Agency. From 1st to 2nd Generation biofuels technologies: an overview of current industry and RD & D activities. 2008. http://www.iea.org/publications/freepublications/publication/2nd_Biofuel_Gen_Exec_Sum.pdf [accessed 25/08/2014].
- [4] Naik SN, Goud VV, Rout PK, Dalai AK. Production of first and second generation biofuels: a comprehensive review. *Renewable and Sustainable Energy Reviews* 2010; 14:578-597. doi:10.1016/j.rser.2009.10.003.
- [5] Food and Agriculture Organization of the UN. FAO food price index. 2013. <http://www.fao.org/worldfoodsituation/foodpricesindex/en/> [accessed 01/09/2014].
- [6] Furimsky E. Hydroprocessing challenges in biofuels production. *Catalysis Today* 2013;217:13-56. doi:<http://dx.doi.org/10.1016/j.cattod.2012.11.008>.
- [7] Bridgwater AV. Principles and practice of biomass fast pyrolysis processes for liquids. *J Anal Appl Pyrolysis* 1999; 51:3-22. doi:[http://dx.doi.org/10.1016/S0165-2370\(99\)00005-4](http://dx.doi.org/10.1016/S0165-2370(99)00005-4).
- [8] Bridgwater AV, Meier D, Radlein D. An overview of fast pyrolysis of biomass. *Org Geochem* 1999; 30:1479-93. doi:[http://dx.doi.org/10.1016/S0146-6380\(99\)00120-5](http://dx.doi.org/10.1016/S0146-6380(99)00120-5).
- [9] Bridgwater AV. Review of fast pyrolysis of biomass and product upgrading. *Biomass Bioenergy* 2012; 38:68-94. doi:<http://dx.doi.org/10.1016/j.biombioe.2011.01.048>.
- [10] Furimsky E. Catalytic hydrodeoxygenation. *Applied Catalysis A: General* 2000; 199:147-90. doi:[http://dx.doi.org/10.1016/S0926-860X\(99\)00555-4](http://dx.doi.org/10.1016/S0926-860X(99)00555-4).
- [11] Carlson T, Vispute T, Huber G. Green Gasoline by Catalytic Fast Pyrolysis of Solid Biomass Derived Compounds. *ChemSusChem* 2008; 1:397-400. doi:10.1002/cssc.200800018.

- [12] Wang X, Kresten SRA, Prins W, Van Swaaij PMW. Biomass Pyrolysis in a Fluidized Bed Reactor. Part 1: Literature Review and Model Simulations. *Ind Eng Chem Res* 2005;- 8773-8785. doi:- 10.1021/ie0504856.
- [13] Gregoire CE, Bain RL. Technoeconomic analysis of the production of biocrude from wood. *Biomass Bioenergy* 1994; 7:275-83. doi:[http://dx.doi.org/10.1016/0961-9534\(94\)00069-6](http://dx.doi.org/10.1016/0961-9534(94)00069-6).
- [14] Cottam M-, Bridgwater AV. Techno-economic modelling of biomass flash pyrolysis and upgrading systems. *Biomass Bioenergy* 1994; 7:267-73. doi:[http://dx.doi.org/10.1016/0961-9534\(94\)00068-5](http://dx.doi.org/10.1016/0961-9534(94)00068-5).
- [15] Islam MN, Ani FN. Techno-economics of rice husk pyrolysis, conversion with catalytic treatment to produce liquid fuel. *Bioresour Technol* 2000; 73:67-75. doi:[http://dx.doi.org/10.1016/S0960-8524\(99\)00085-1](http://dx.doi.org/10.1016/S0960-8524(99)00085-1).
- [16] Mullaney H, Farag H, LaClaire C, Barrett C. Technical, Environmental and Economic Feasibility of Bio-Oil in New Hampshire's North Country. 2002; 14B316 UDKEIF.
- [17] Jones S, Valkenburg C, Walton C, Elliott D, Holladay J, Stevens D, et al. Production of gasoline and diesel from biomass via fast pyrolysis, hydrotreating and hydrocracking: a design case; PNNL-18284. Richland, WA (US): Pacific Northwest National Laboratory (PNNL); 2009.
- [18] Wright MM, Daugaard DE, Satrio JA, Brown RC Techno-economic analysis of biomass fast pyrolysis to transportation fuels. *Fuel* 2010; 89, Supplement 1:S2-S10. doi:10.1016/j.fuel.2010.07.029.
- [19] Ranzi E, Faravelli T, Frassoldati A, Migliavacca G, Pierucci S, Sommariva S. Chemical kinetics of biomass pyrolysis. *Energy Fuel* 2008;22:4292–300.
- [20] Wang X, Kresten SRA, Prins W, Van Swaaij PMW. Biomass Pyrolysis in a Fluidized Bed Reactor. Part 2: Experimental Validation of Model Results. *Ind Eng Chem Res* 2005;- 8786-8795. doi:- 10.1021/ie050486y.
- [21] Sheu YE, Anthony RG, Soltes EJ. Kinetic studies of upgrading pine pyrolytic oil by hydrotreatment. *Fuel Process Technol* 1988; 19:31-50. doi:[http://dx.doi.org/10.1016/0378-3820\(88\)90084-7](http://dx.doi.org/10.1016/0378-3820(88)90084-7).
- [22] Li H, Chen Q, Zhang X, Finney KN, Sharifi VN, Swithenbank J. Evaluation of a biomass drying process using waste heat from process industries: A case study. *Appl Therm Eng* 2012; 35:71-80. doi:<http://dx.doi.org/10.1016/j.applthermaleng.2011.10.009>.
- [23] Fournol AB, Bergougnou MA, Baker CGJ. Solids entrainment in a large gas fluidized bed. *The Canadian Journal of Chemical Engineering* 1973; 51:401-4. doi:10.1002/cjce.5450510402.
- [24] Marker TL. Opportunities for biorenewables in oil refineries. Final Technical Report. United States. 2005; DOEGO15085.

- [25] Elliott DC, Hart TR, Neuenschwander GG, Rotness LJ, Zacher AH. Catalytic hydroprocessing of biomass fast pyrolysis bio-oil to produce hydrocarbon products. *Environmental Progress & Sustainable Energy* 2009; 28:441-9. doi:10.1002/ep.10384.
- [26] Biomass Energy Centre. Fuel cost per kWh. http://www.biomassenergycentre.org.uk/portal/page?_pageid=75,59188&_dad=portal [Accessed 25/08/2014]
- [27] Sigma-Aldrich. Platinum on alumina. <http://www.sigmaaldrich.com/catalog/product/aldrich/205974?lang=en®ion=GB> [Accessed 25/08/2014]
- [28] ECN Phyllis2. Database for biomass and waste. <https://www.ecn.nl/phyllis2/Browse/Standard/ECN-Phyllis> [Accessed 25/08/2014]

TABLES

Table 1 Process assumptions

Process Section	Process Assumption
 Pretreatment(A100)	Biomass size as received is 20mm with 25% initial moisture content.

	Fast Pyrolysis(A200)	Process heat supplied by NCG and char combustion with nitrogen as the fluidizing gas.	
	Solid Removal(A300)	Solid products are separated from the hot vapours stream by high efficiency cyclones at 95% separation efficiency.	
	Bio-oil Recovery(A400)	A direct contact spray tower used for rapid quenching of bio-vapours to 49°C using previously stored bio-oil as quench liquid.	
	Combustion(A500)	Char is combusted in 60% theoretical air to obtain 1269°C to prevent ash melting at adiabatic flame temperature up to 1700°C	
	Power Generation (A600)	Steam Rankine cycle with an isentropic efficiency of 75% and turbine efficiency of 85%.	
upgrading	Bio-oil	Bio-oil upgrading (A700)	2 stage hydrotreating reactions over Pt/Al ₂ O ₃ /SiO ₂ catalysts.
		Hydrogen Generation(A800)	Hydrogen generated from the reforming of bio-oil aqueous phase and supplementary natural gas.

Table 2 Cost inputs and assumptions

Parameter	Value	Parameter	Value
Pine wood cost (£/ton)[26]	90	Annual RRR (%)	10
5 wt.% Pt/Al ₂ O ₃ catalyst cost (£/kg)[27]	4,500	Project Contingency (%)	20
Ash disposal cost (£/ton)[18]	0.11	Project economic life (year)	20
Supplementary natural gas (£/GJ)	3.59	Working Capital (%)	5

Electricity price ((£/kWh)[26]	0.15	Depreciation method	Straight Line
PSA operating cost (£/ton)	21	Plant Overhead (%)	50
Project Capital and Product Escalation (%)	5.00	Operating Cost Escalation (%)	3

Table 3 Proximate and chemical composition of pine wood [28]

Proximate Analysis	wt.%	Subcomponent Composition	wt.%
Moisture content	25	Cellulose	42
Fixed Carbon	20	Hemicellulose	23
Volatile Matter	55	Lignin	24

Ash	0.7	Water	10
-----	-----	-------	----

Table 4 Pyrolysis chemical reactions [19]

Reaction		$A(s^{-1})$	E (kJ/mol)
1	Cell \rightarrow CellA	8×10^{13}	192.5

2	Cell → 5H ₂ O + 6 Char	8 x 10 ⁷	125.5
3	CellA → Levoglucosan	4T	41.8
4	CellA → 0.95HAA +0.25Glyoxal +0.2Acetaldehyde+0.25HMFU+ 0.2Acetone+0.16CO ₂ + 0.23CO+0.9H ₂ O+0.1CH ₄ +0.61Char	1 x 10 ⁹	133.9
5	HCell → 0.4HCell1 +0.6 HCell2	1 x 10 ¹⁰	12.9.7
6	HCell → 0.75H ₂ +0.8CO ₂ +1.4CO + 0.5Formaldehyde	3 x 10 ⁹	113
7	HCell1 → Xylan	3T	46
8	HCell2 → CO ₂ + 0.5CH ₄ +0.25 C ₂ H ₄ + 0.8CO + 0.8H ₂ +0.7Formaldehyde+0.25 Methanol +0.125Ethanol + 0.125H ₂ O +Char	1 x 10 ¹⁰	138.1
9	Lig _C →0.35Lig _{CC} + 0.1pCourmaryl + 0.08Phenol + 0.14C ₂ H ₄ + H ₂ O + 0.495CH ₄ + 0.32CO ₂ + CO+ H ₂ + 5.735Char	4 x 10 ¹⁵	202.9
10	Lig _H → LigOH +Acetone	2 x 10 ¹³	156.9
11	Lig _O →LigOH +CO ₂	1 x 10 ⁹	106.7
12	Lig _{CC} →0.3pCoumaryl + 0.2Phenol + 0.35Acrylic + 0.7H ₂ O + 0.65CH ₄ + 0.6C ₂ H ₄ + 1.8CO + H ₂ + 6.4Char	5 x 10 ⁶	131.8
13	Lig _{OH} → Lig + H ₂ O + Methanol + 0.45CH ₄ + 0.2C ₂ H ₄ + 2CO + 0.7H ₂ + 4.15Char	3x 10 ⁸	125.5
14	Lig → Lumped Phenol	8T	50.2
15	Lig → H ₂ O +2CO+0.2Formaldehyde +0.4Methanol +0.2Acetaldehyde +0.2 Acetone+0.6CH ₄ + 0.65C ₂ H ₄ + 0.5H ₂ + 5.5Char	1.2x 10 ⁹	125.5

Table 5 Bio-oil hydrotreating reactions [21]

Reaction	A(s ⁻¹)	E (kj/mol)
----------	---------------------	------------

1	Heavy non-volatiles → Light non-volatile	6.40 x 10	78
2	Heavy non-volatiles → [Alkanes + Aromatics]	1.26 x 10 ³	91.8
3	Light non-volatiles → Phenolics	1.38 x 10 ²	80.6
4	Phenolics → [Alkanes + Aromatics]	1.58 x 10	62.3
5	[Alkanes + Aromatics] → [Coke + Water + Gases]	7.75 x 10	75

Table 6 Pyrolysis model validation with experimental measurements at 500 °C

Pyrolysis products	Model (wt. %)	Experiment[20] (wt. %)	Relative error (%)
Gas	21	21.5	2.33%
Bio-oil	65	64	1.56%
Char	14	14.5	3.45%

Table 7 Hydrotreated bio-oil results validated with experimental measurements

Lumped bio-oil components	HT Model (wt. %)	Experiment [21] (wt. %).	Relative error (%)
Heavy nonvolatiles	22.94	24.57	6.64%
Light nonvolatiles	29.83	29.41	1.41%
Phenolics	10.55	10.63	0.76%
[Aromatics +Alkanes]	19.82	19.52	4.33%
Gases + H ₂ O + Coke	16.86	15.87	5.40%

Table 8 Stream summary of whole process

Component (wt. %)	Dried Biomass	Dryer Exhaust	NCG	Bio-oil	Char	Fuel
Nitrogen	-	73.45	80.90	0.03	-	-
Oxygen	-	21.94	-	-	-	-
Hydrogen	-	-	0.32	0.00	-	-
Methane	-	-	1.71	0.00	-	-
Ethylene	-	-	1.63	0.01	-	-
Carbon monoxide	-	-	6.22	0.00	-	-
Carbon dioxide	-	-	6.20	0.03	-	-
Water	-	4.61	0.19	20.55	-	-
Levoglucosan	-	-	-	48.23	-	-
HAA	-	-	0.00	3.29	-	-
Glyoxal	-	-	0.20	0.45	-	-
Acetaldehyde	-	-	0.29	0.03	-	-
HMFU	-	-	-	1.82	-	-
Acetone	-	-	0.84	0.47	-	-
Acrylic	-	-	0.00	0.01	-	-
Xylan	-	-	-	0.36	-	-
Formaldehyde	-	-	1.35	2.06	-	-
Phenol	-	-	0.00	0.74	-	-
Methanol	-	-	0.00	2.71	-	-
Ethanol	-	-	0.16	1.12	-	-
pCoumaryl	-	-	0.00	1.48	-	-
L-Phenol	-	-	0.00	1.37	-	-
Naphthenes	-	-	-	-	-	70.00
Aromatic	-	-	-	-	-	12.00
n/i-Alkanes	-	-	-	-	-	18.00
Cellulose	-	-	-	-	27.43	-
Hemicellulose	-	-	-	2.15	5.39	-
Lignin Derivatives	-	-	-	12.43	1.28	-
Biomass	100	-	-	-	-	-
Char	-	-	0.00	0.65	60.14	-
Ash	-	-	0.00	0.00	5.76	-
Total Mass flow (kg/hr)	2,489	10,833	3,090	1,597	303	503

Table 9 Composition of various biomasses [28]

Component	Pine wood	Switch grass	Poplar	Pine bark
Cellulose	0.42	0.36	0.47	0.22
Hemicellulose	0.23	0.31	0.22	0.23
Lignin	0.24	0.18	0.20	0.47
Water	0.10	0.10	0.10	0.06
Ash	0.01	0.05	0.01	0.02

Table 10 Economic results

Parameter	Value
Plant Size MT/day)	72
Total Capital Investment (£ MM)	16.6
Annual Operating Cost (£ MM)	6.4
Fuel Yield (MMGGE/Year)	1.8
Product Value (£ /GGE)	6.69

FIGURES

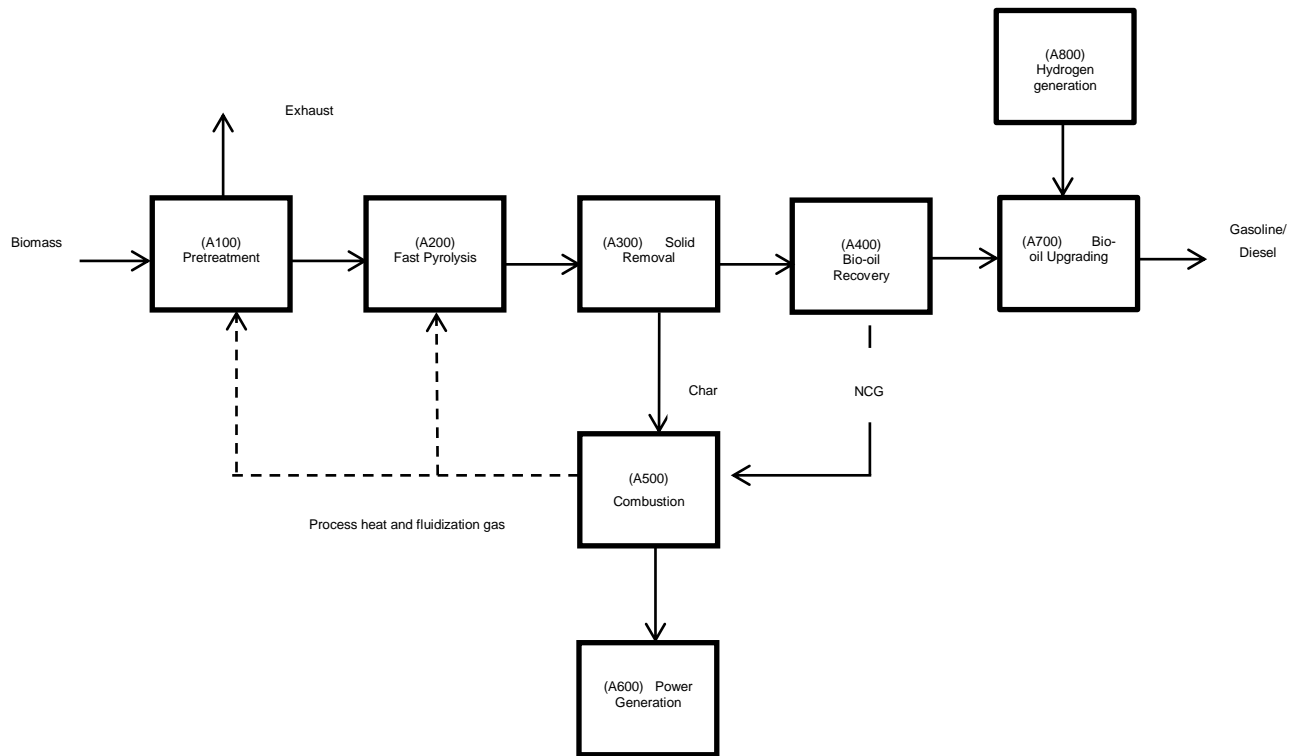


Figure 1 Generalised process flow diagram

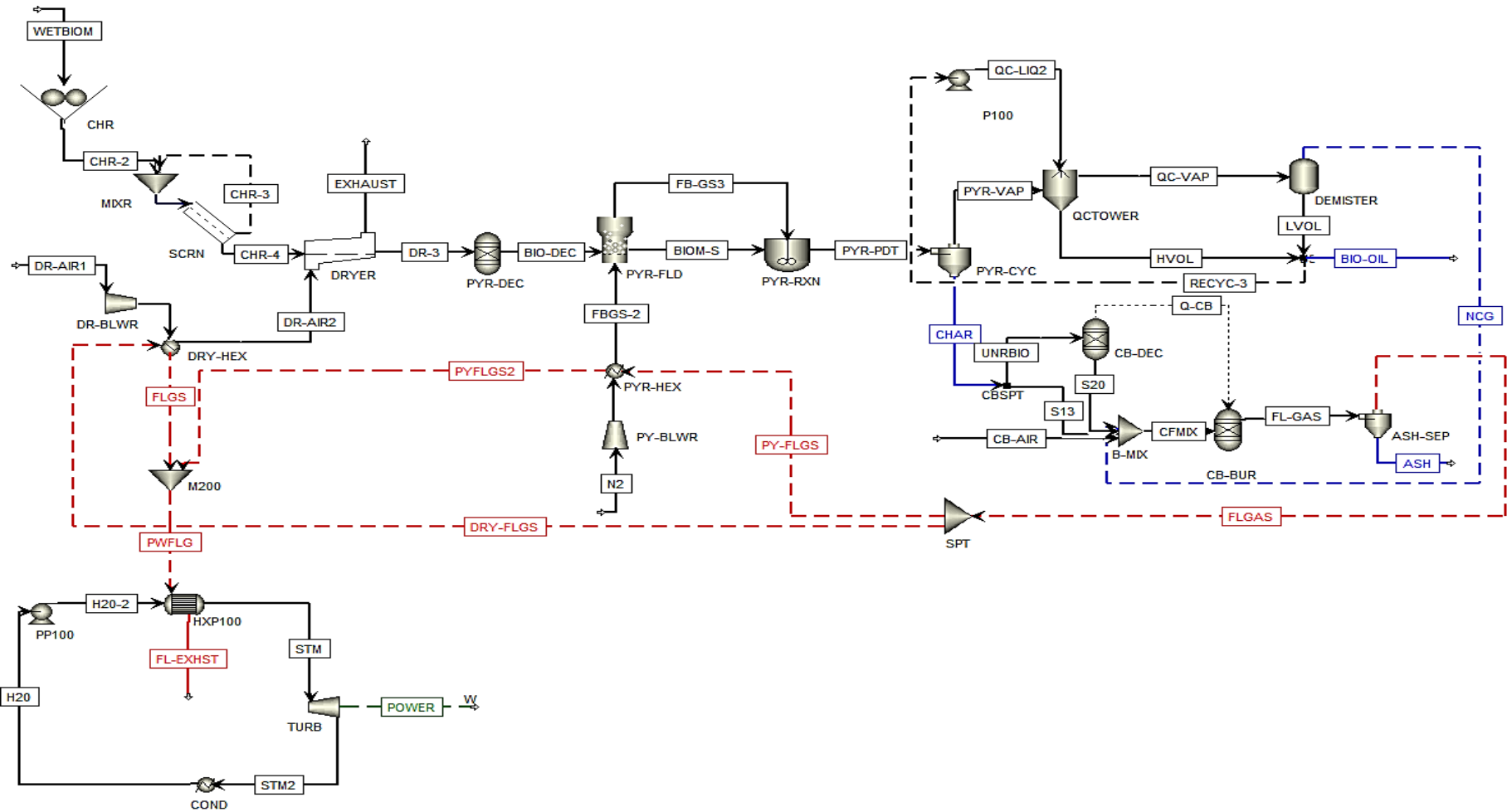


Figure 2 Fast pyrolysis process flowsheet (A100- A600)

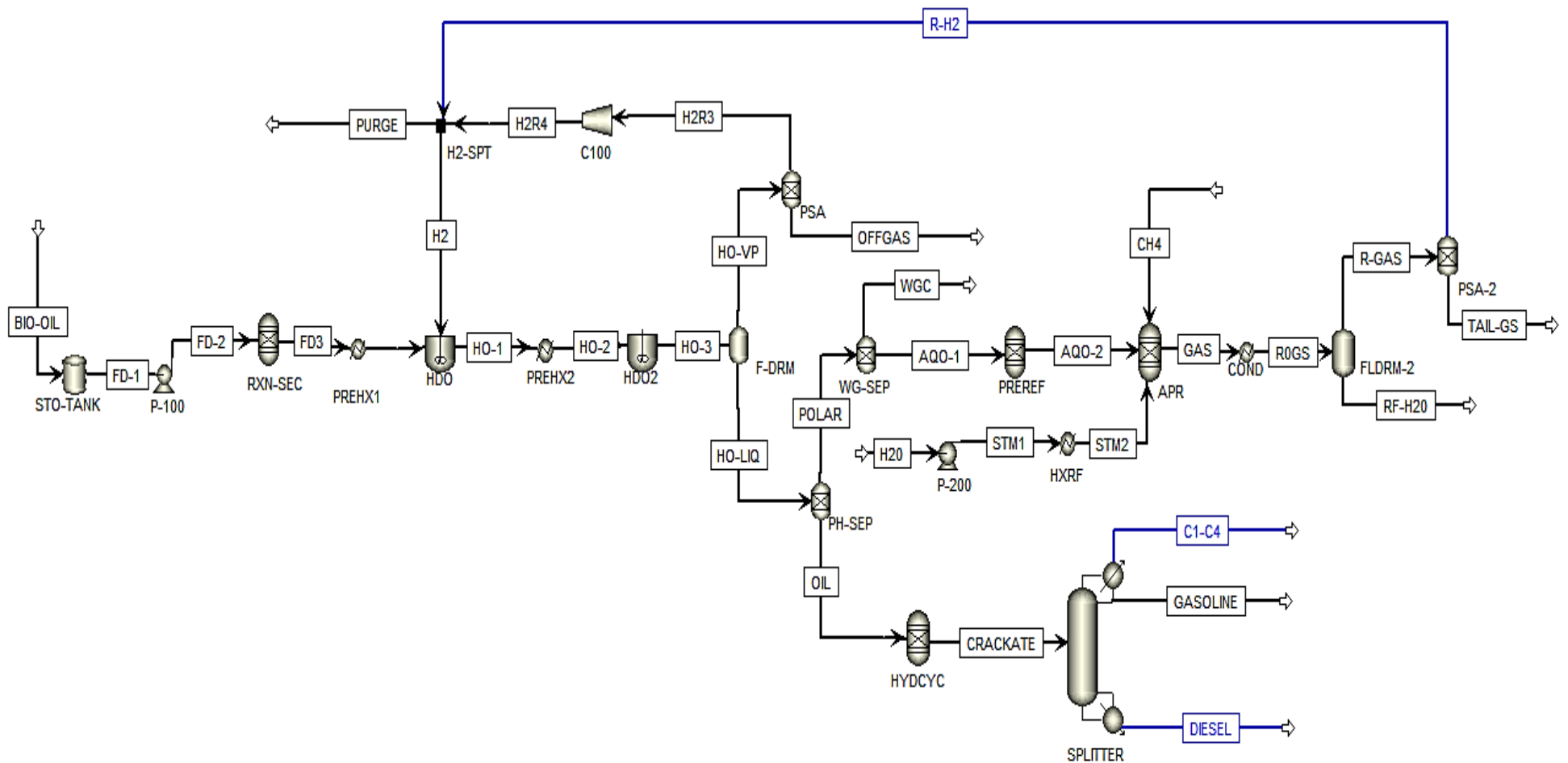
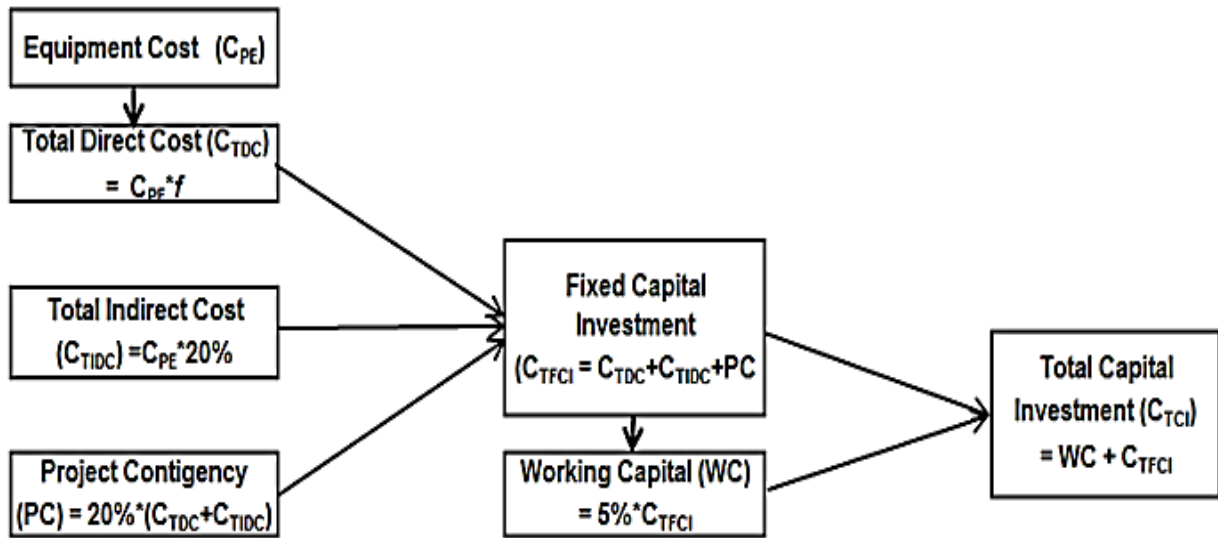


Figure 3 Bio-oil hydroprocessing and hydrogen production (A700 – A800)



f = installation factor

Figure 4 Capital investment estimation methodology

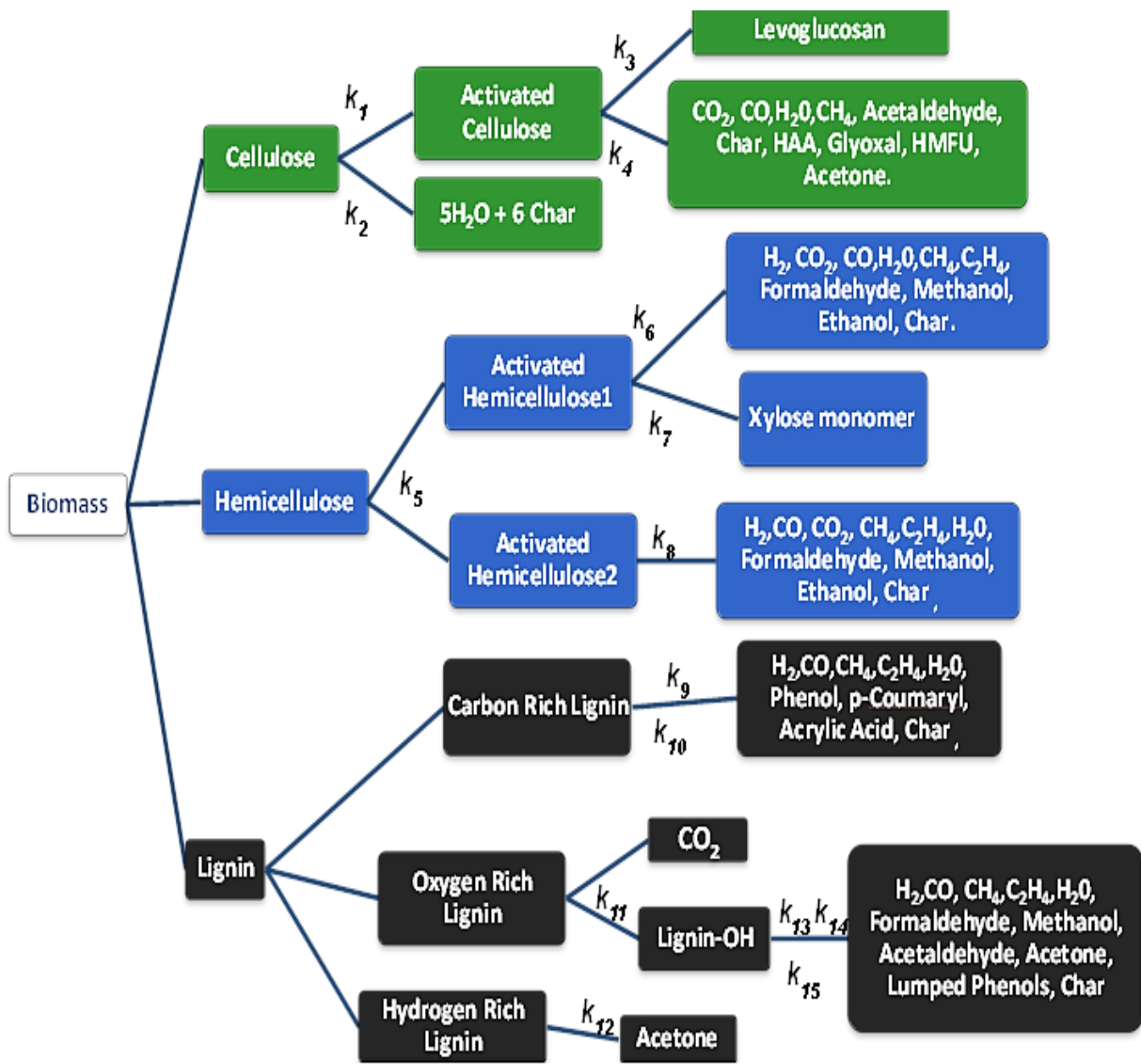


Figure 5 Multi-step reaction kinetics of biomass pyrolysis [19]

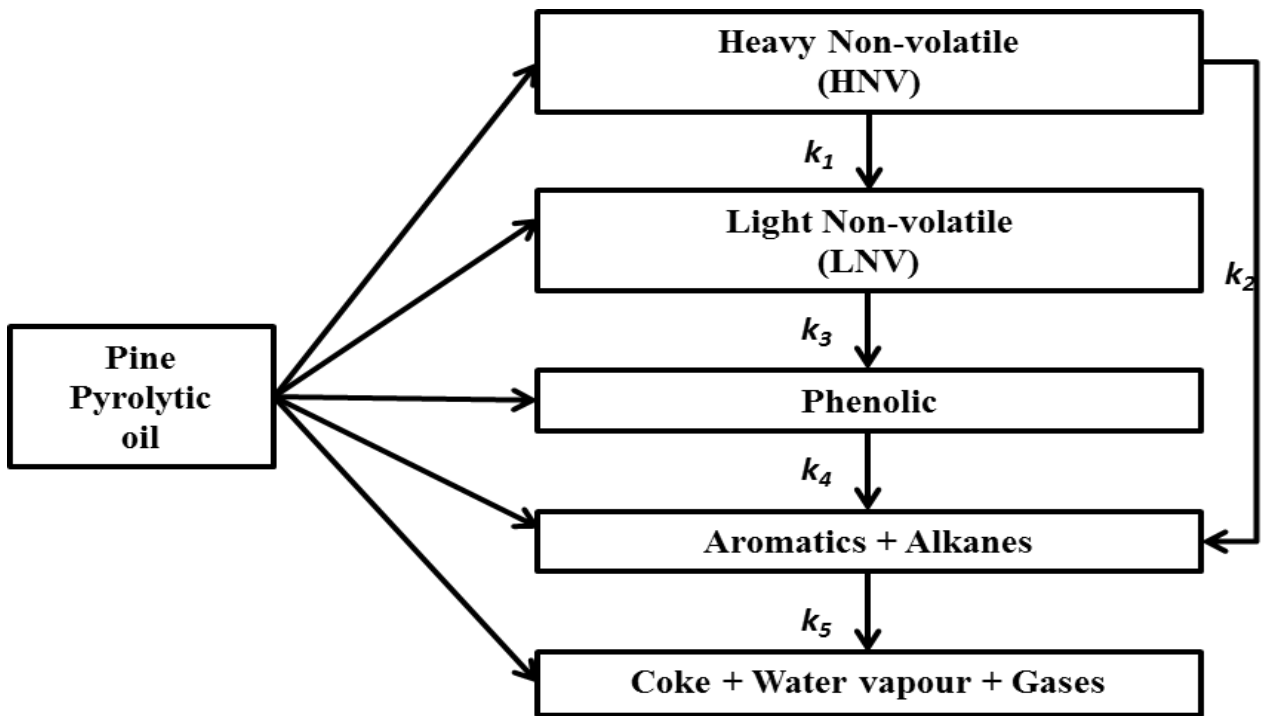


Figure 6 Reaction kinetic model of lumped bio-oil species

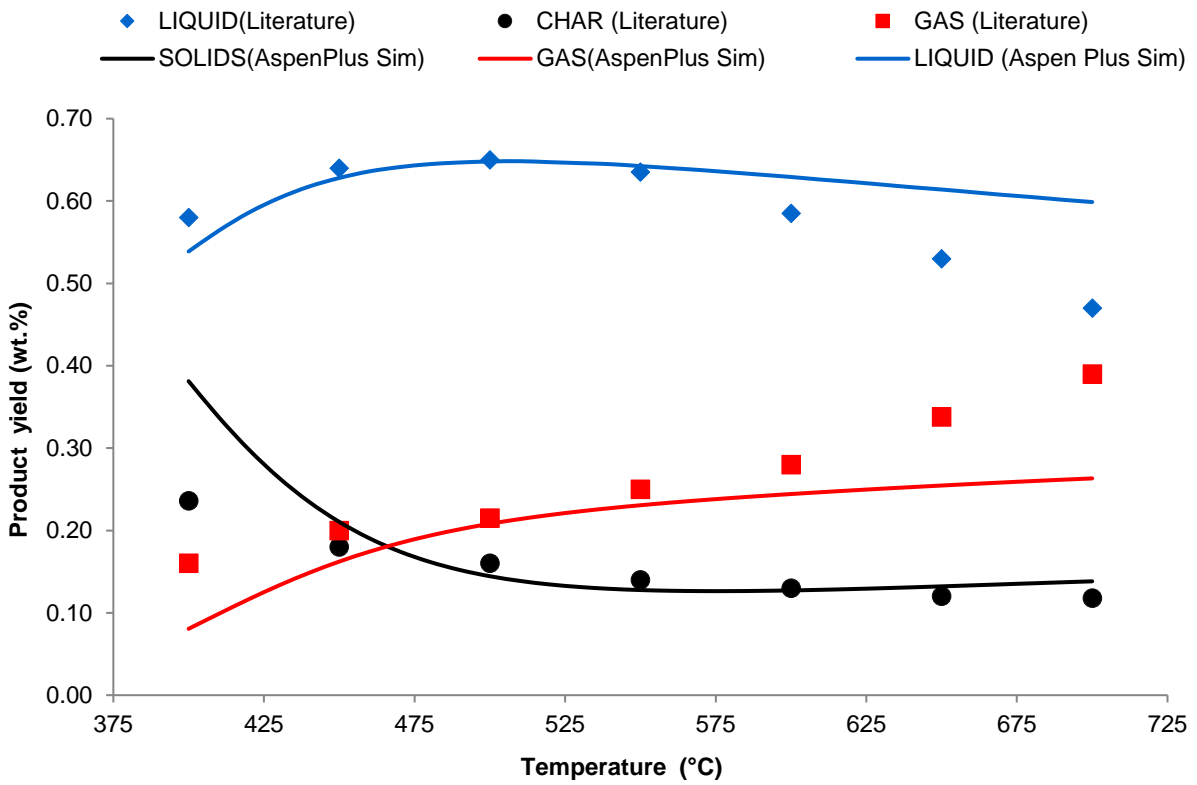


Figure 7 Aspen plus simulation results vs. experimental data from [20] as a function of reactor temperature

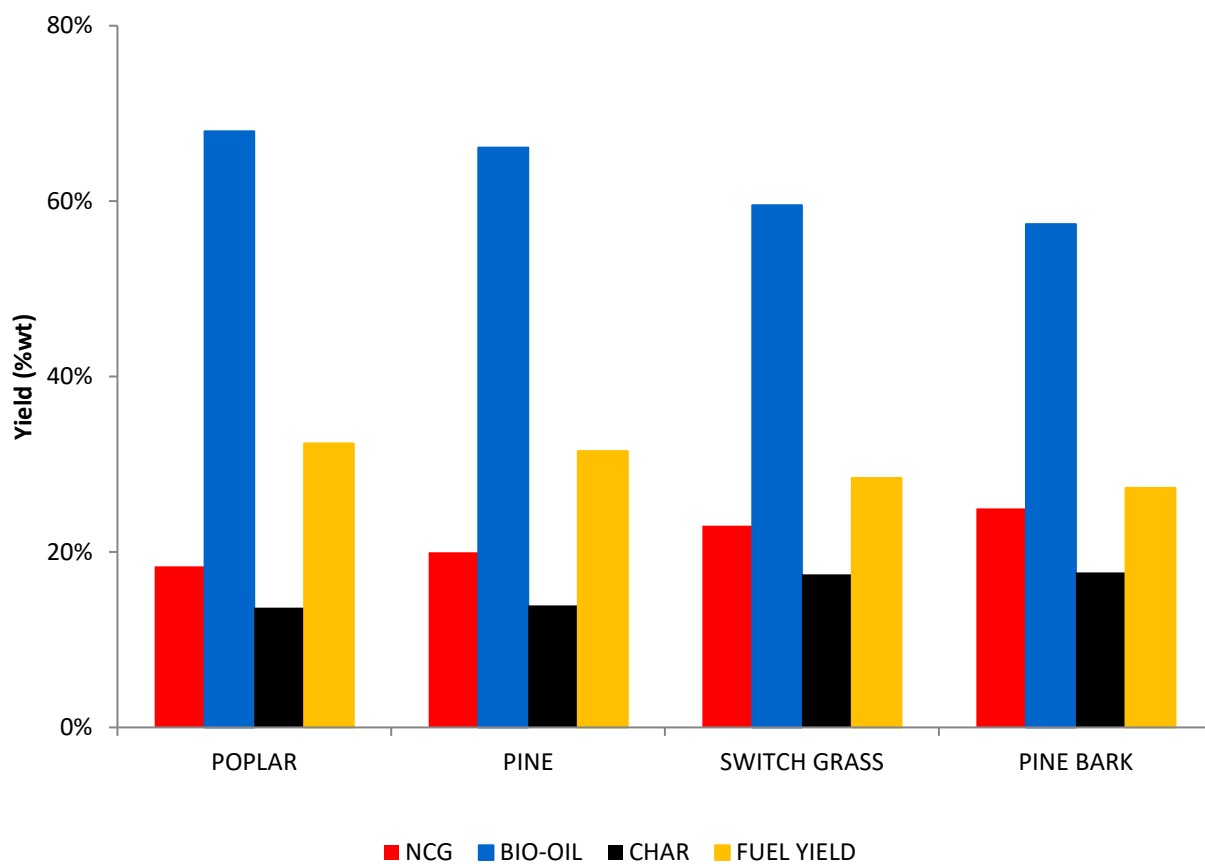


Figure 8 Fast pyrolysis products and biofuel yield from various biomasses

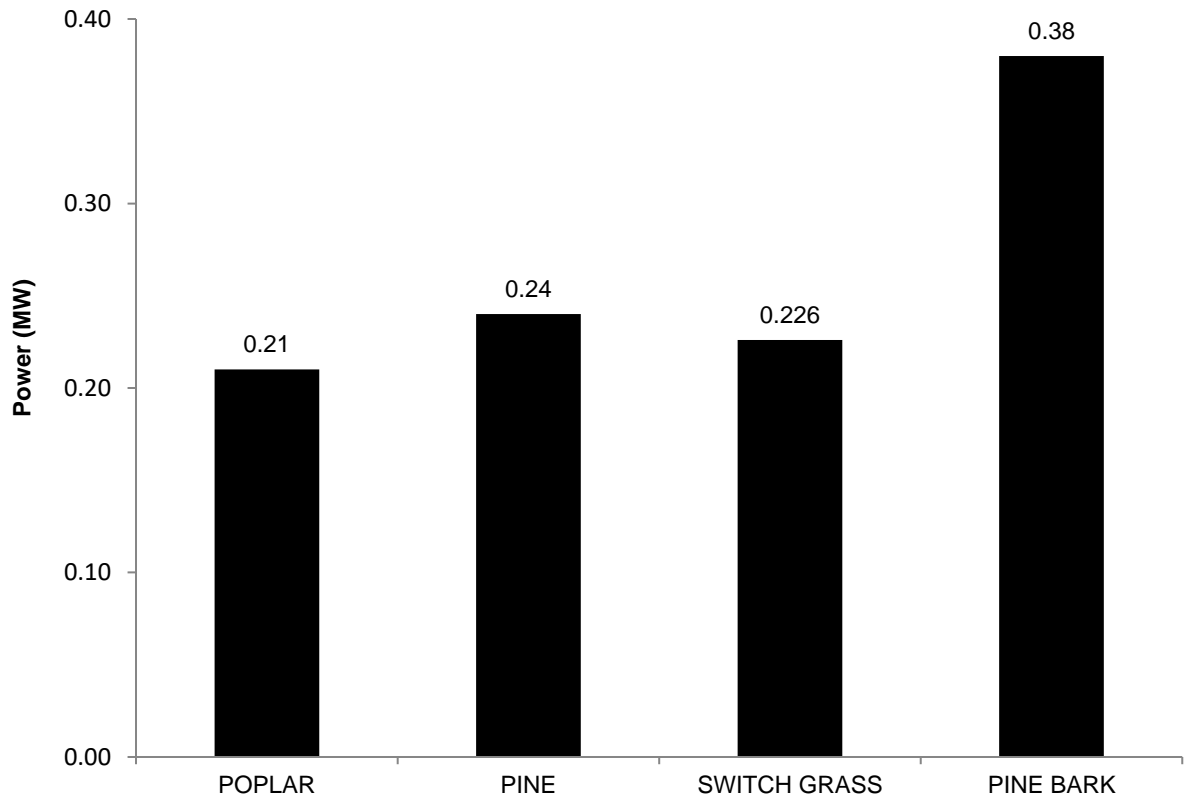


Figure 9 Electric power generated from various biomass

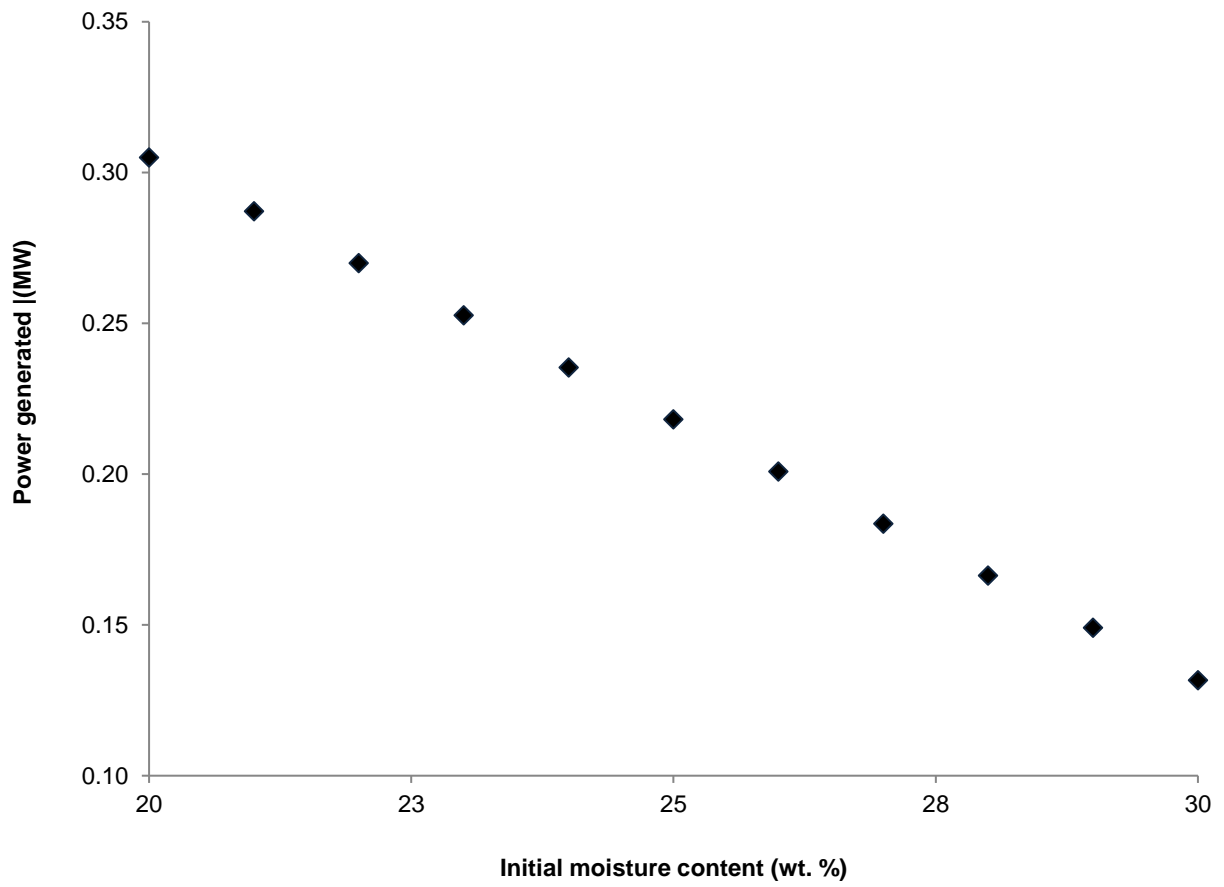


Figure 10 Effect of initial moisture content in biomass on power generated in the process

Total Capital Investment

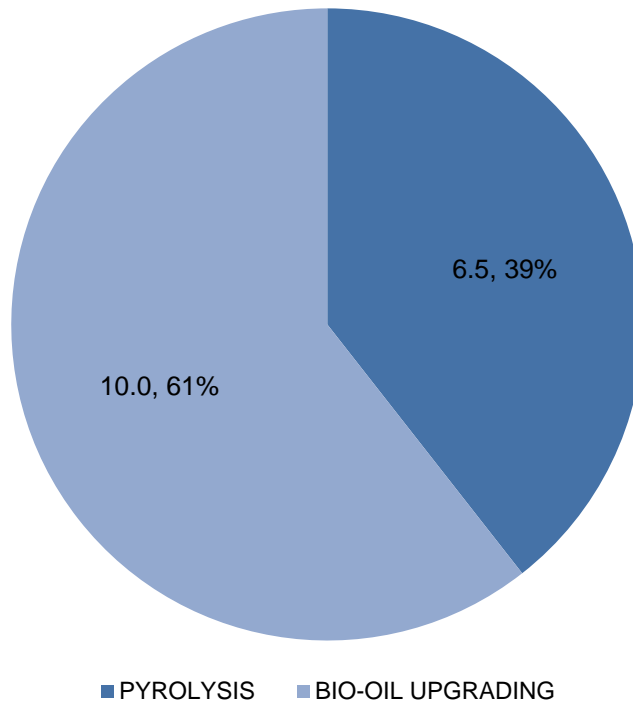


Figure 11 Total capital investment of the two main sub-processes

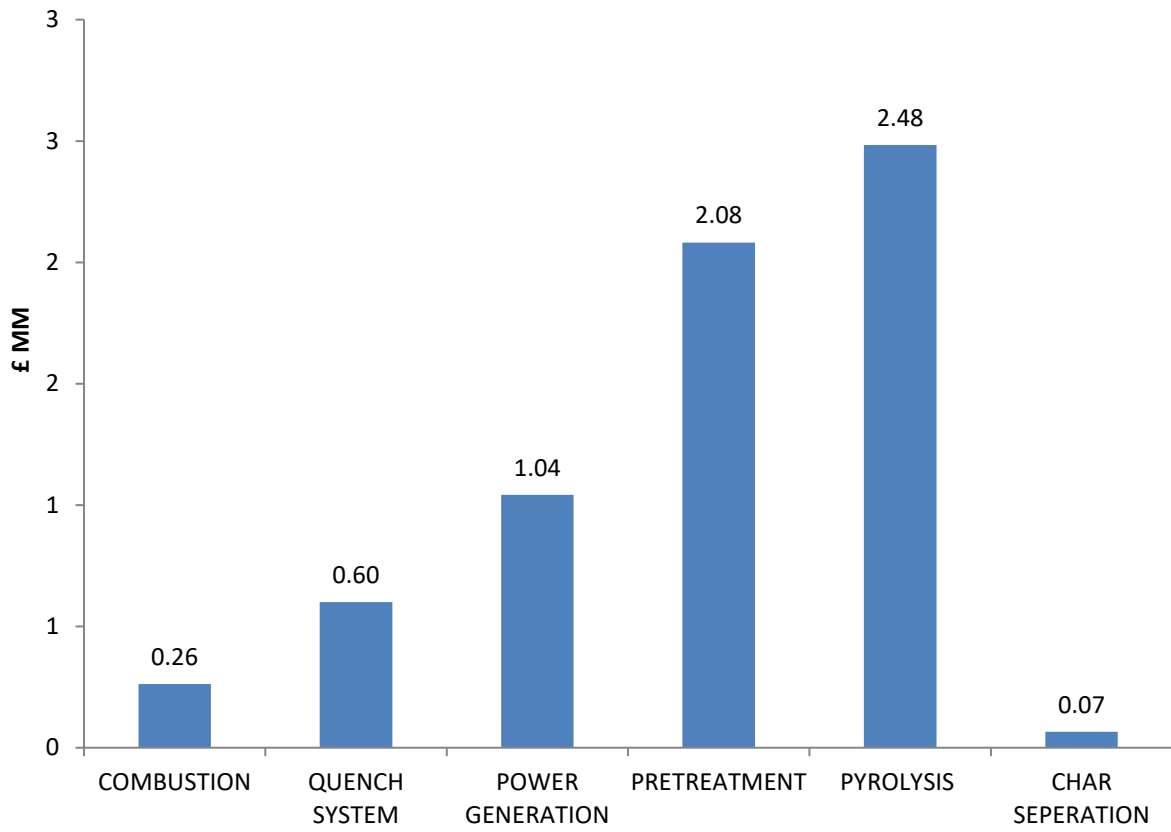


Figure 12 Total capital investment distribution of pyrolysis plant

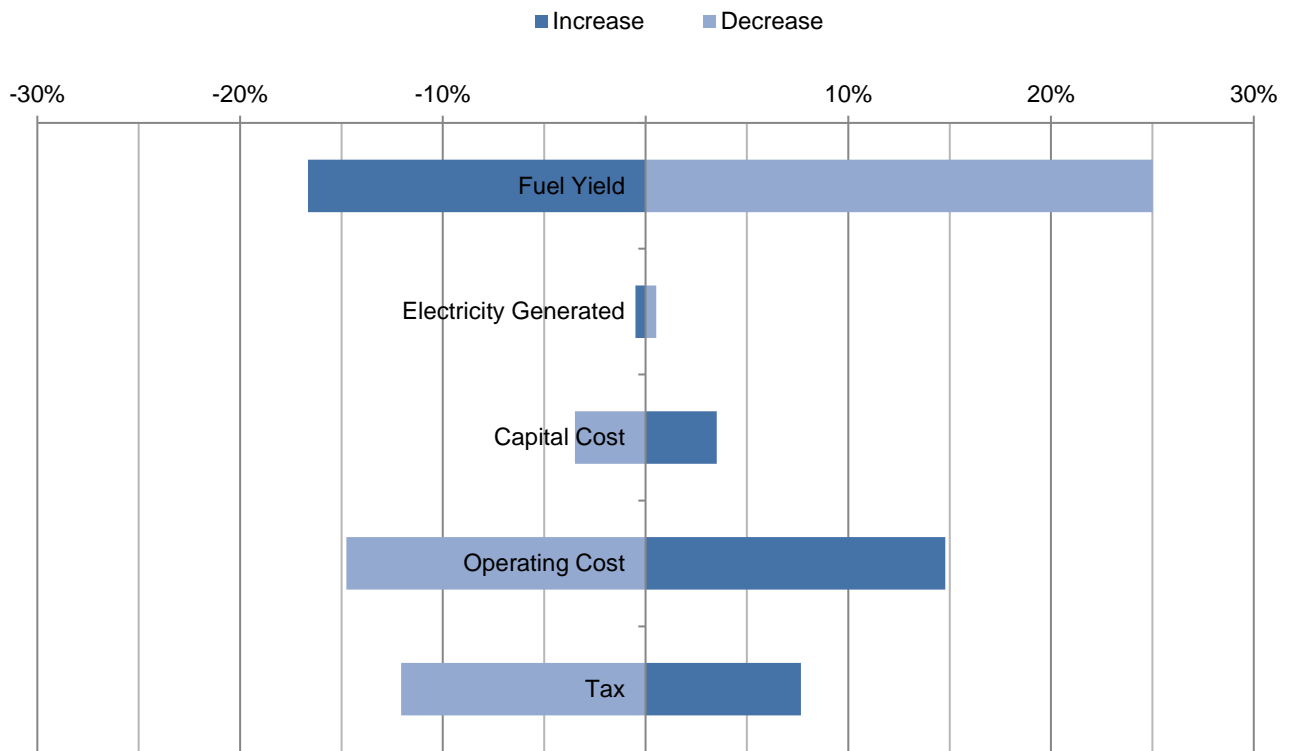


Figure 13 Percentage difference in fuel product value over a $\pm 20\%$ change (increase/decrease) in process and economic parameters

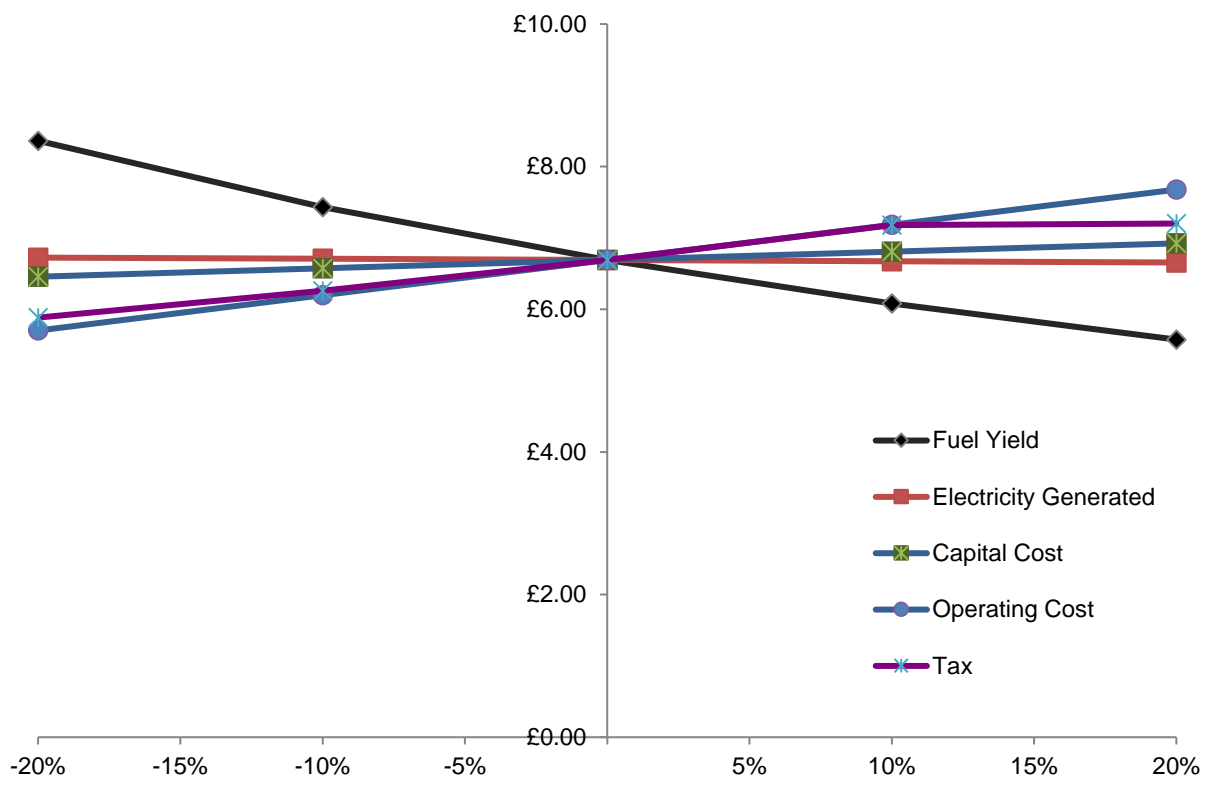


Figure 14 Fuel product value sensitivity to process and economic parameters